

Tool for detecting waveform distortions in inverter-based Microgrids: a validation study

Geir Kulia

Department of Electronics and
Telecommunications,
NTNU,
7491 Trondheim,
Email: geir.kulia.1991@ieee.org

Marta Molinas

Department of Engineering Cybernetics,
NTNU,
7491 Trondheim,
Email: marta.molinas@ieee.org

Lars Lundheim

Department of Electronics and
Telecommunications,
NTNU,
7491 Trondheim,
Email: lundheim@iet.ntnu.no

Abstract—This paper presents a validation methodology based on data analysis aimed at identifying the cause of atypical behavior observed in a microgrid’s data. The data of a stand-alone PV microgrid in Bhutan is used for the analysis. Voltage waveform distortions observed in the data were analyzed by utilizing the Hilbert-Huang Transform (HHT) and the discrete Fourier transform (DFT). When using HHT, a time-varying frequency, new to electrical systems, is revealed by the microgrid data analysis, while the mathematical derivation hints on amplitude modulation. The distortions appeared in the form of a leakage spectrum composed of multiple numbers of constant frequency components when using a DFT-based frequency power spectrum. The different observations from these methods have raised questions of interpretation of their physical meaning. In an attempt to provide a physical meaning and to understand the cause of the time varying frequency revealed by the HHT, an analytical investigation of the microgrid controller is performed. The results obtained indicate that modern power electronics introduces new types of distortions that can be traced back to the control of the inverters in the microgrid. The analytically obtained results compared with the analysis of simulated and field measurements hint on the existence of a time-varying frequency in the voltage waveforms of the stand-alone microgrid. The results of this paper will lay the foundation for future studies into more accurate diagnosis tools for microgrids to enable affordable access to electricity in isolated communities.

Keywords—*Instantaneous frequency, Fourier Transform, Hilbert-Huang Transform, Empirical Mode Decomposition, Microgrid, Single-phase Inverter, Amplitude modulation, Frequency stability, Steady-State, power electronics.*

I. MOTIVATION

Universal access to affordable modern power services is one of the United Nations sustainable development goals [2]. Electrical power is the foundation of modern business, medicine, education, agriculture, infrastructure, and communications. Lack of electrical energy is, therefore, a severe impediment to economic growth, yet, this is the case for 1.2 billion people worldwide. Of these 1.2 billion without electricity access, 80 % lives in rural areas; 95 % in sub-Saharan Africa or in developing Asia [3]. Applying islanded microgrids with free renewable energy sources is an alternative for providing electricity to isolated communities where extending the main grid is too expensive. Microgrids



Fig. 1: ACME Portables FlexPAC, the core component in the prototype of the real-time analysis device for microgrids based on instantaneous frequency [1].

are electrical systems that locally generate, store and provide power to a small area, such as a village. Traditionally, these grids have often been based on diesel aggregates, but due to the recent fall in prices for photovoltaic (PV) cells, PV based microgrids have become a conspicuous substitute that can provide cleaner and cheaper electricity.

Because of the nature of the location for where the islanded microgrids are desirable, the microgrids needs to be near to maintenance free and have a supervisory control system that can handle any faults that might occur. Due to the stochastic nature of PV sources and the nonlinearities of modern power electronic equipment that are essential microgrid components, the need for accurate monitoring and diagnosis devices based on measurement of instantaneous values of fundamental electrical parameters rather than average values has become apparent. The authors are currently developing a prototype for a real-time monitoring and diagnosis device for detecting the instantaneous frequency and time-dependent distortions due to nonlinearities. The development is carried out by the authors and a team of students and interns at the Norwegian University of Science and Technology (NTNU). Fig. 1 shows a photo of the prototype. This initiative is part of a greater partnership with the Royal University of Bhutan (RUB)s College of Science and Technology (CST) that

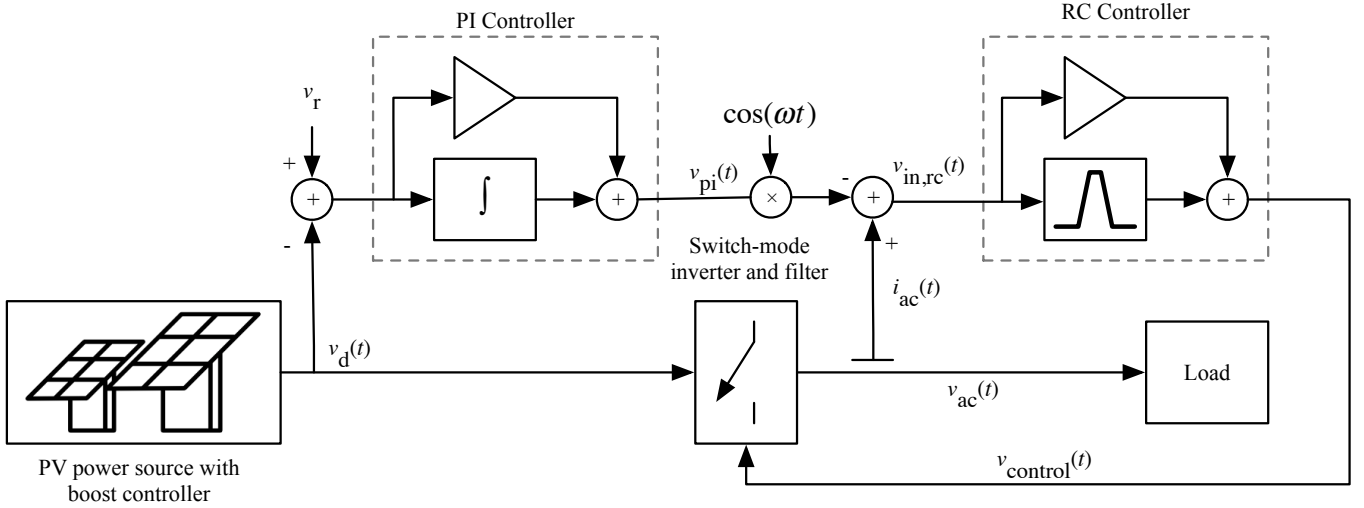


Fig. 2: High level model of the microgrid investigated in this paper

aim at developing reliable and affordable solutions for easy diagnosis and correction of potential problems of microgrids in rural areas.

In a previous contribution, the authors presented a method for decomposing and analyzing electrical voltage and current waveforms to estimate the instantaneous frequency [4] by applying the Hilbert-Huang Transform [5]. We then suggested that the electrical waveforms were frequency modulated, of considerable magnitude. This paper presents a validation study for a diagnosis tool for microgrids based on the investigation of the system behind the microgrid and its controllers. The validation procedure is based on providing first an analytical model of the distortion, supported by simulation data from a detailed Matlab model which then are used to discuss and validate the results observed in the field data. The results from the analytical model and the simulation model exhibit seemingly non-periodic properties of the instantaneous frequencies when compared with the measured waveforms obtained at RUB CST's stand-alone microgrid. The expected grid frequency in such systems should be a stationary 50 Hz, while the observed frequencies in this investigation show a distorted oscillatory frequency with cycles of 10 ms on the grid frequency.

By better understanding the root cause of the phenomena behind the distortions on the microgrid, we gain better knowledge on how to design and tune the inverters to easier suit the environment where they will be applied. The authors hope this can help to lay a foundation of a methodology to diagnose microgrids so that we can contribute to providing more reliable and less maintenance demanding electricity access to rural areas in the developing world.

II. PROBLEM IDENTIFICATION THROUGH ANALYTICAL MODELLING

The authors have previously identified unexpected distortions on a stand-alone microgrid [4]. By reverse engineering the

system from the observed data, the impact of the inverter controller will be identified. This section will present the hypothesis and the results of the reverse engineering exercise. The analytical approach and the assumptions made will be compared with a simulation and field measurement of voltage waveforms.

Fig. 2 shows a model of the microgrid. In the model, the dc voltage $v_d(t)$ is supplied from a dc source. The dc voltage $v_d(t)$ is converted to ac, $v_{ac}(t)$, by using a dc/ac inverter. The inverter is a steady-state single bridge inverter based on pulse-width modulation (pwm) [6] with a low-pass filter. The inverter has a controller that uses $v_d(t)$ and the $i_{ac}(t)$ to control $v_{ac}(t)$ so that ideally, the ac output voltage should always be

$$v_{ac}(t) = V_{ac} \cos \omega_o t. \quad (1)$$

where ω_o is the fundamental grid frequency and is constant: $\omega_o = 2\pi \cdot f_o = 2\pi 50$ Hz. $v_{ac}(t)$ is adjusted by $v_{control}(t)$. By assuming a optimal dc/ac inverter and filter, $v_{ac}(t)$ will be

$$v_{ac}(t) \propto v_{control}(t). \quad (2)$$

The inverter controller used in this article is based on a typical PV inverter controller [7], [8]. The frequency and phase-shift synctonization is not accounted for in this paper as the microgrid is islanded. The controller's task is to monitore and correct the output voltage v_{ac} . The controller's main blocks are proportionalintegral (PI) controller and a Resonant Controller (RC) as shown in the fig. 2.

In this paper, a general signal will be written in the form

$$x(t) = X + \tilde{x}(t). \quad (3)$$

This means that X is the constant dc part of $x(t)$, and $\tilde{x}(t)$ is the time-varying ac part of $x(t)$.

The previous study leads us to believe that the distortions originate in an oscillation on the dc bus. By following the

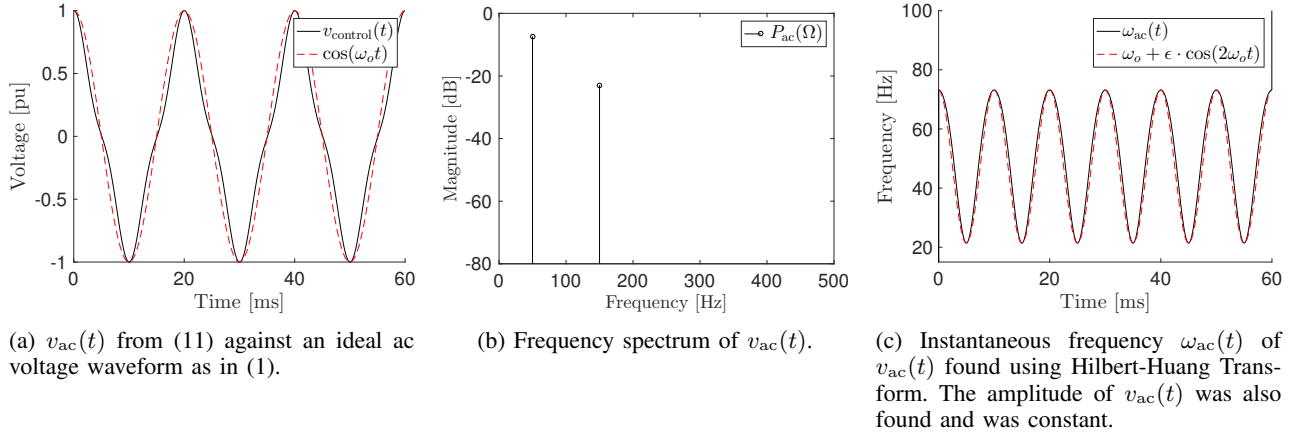


Fig. 3: Analytical representation of $v_{ac}(t)$ together with its frequency power spectrum and Hilbert-Huang transform.

argumentation in app. A; if the load is a resistance, the dc voltage can be modelled as

$$v_d(t) = V_d + \tilde{v}_d(t) = V_d + \tilde{V}_d \cos(2\omega_o t). \quad (4)$$

In the controller, the dc voltage, $v_d(t)$ is compared with a predefined reference dc voltage v_r and results in a correction signal

$$v_e(t) = v_r - v_d(t). \quad (5)$$

We assume a stable boost controller so that the correction signal v_r is equal to V_d . The proportionalintegral controller (PI) uses the correction signal $v_e(t)$ as an input. The purpose of the PI controller is to maintain a stable output amplitude of v_{ac} while there are slow-varying changes in the dc voltage v_d . Since the PI controller is a linear operation, it will only alter the amplitudes and not any frequency component of $v_d(t)$, resulting in an output of the PI controller

$$v_{pi}(t) = A \cos(2\omega_o t - \phi) \quad (6)$$

where A and ϕ are the resulting amplitude and phase after the PI controller. The resulting $v_{pi}(t)$ is used, together with a signal proportional to the ac current to set the frequency for the $v_{in,rc}(t)$ as an input to the resonant controller (RC). Assuming we have a resistive load, we also have that

$$v_{ac}(t) = R_{load} \cdot i_{ac}(t). \quad (7)$$

The expression for the input to the resonant controller $v_{in,rc}(t)$ is then given by

$$\begin{aligned} v_{in,rc}(t) &= -A \cos(2\omega_o t - \phi) \cdot \cos(\omega_o t) + B' \cdot v_{ac} \\ &= -\frac{A}{2} (\cos(\omega t - \phi) + \cos(3\omega t - \phi)) + B' \cdot v_{ac}(t) \end{aligned} \quad (8)$$

where B' is a constant to scale $v_{ac}(t)$. The Resonant Controller is a linear band amplifier that let all frequencies pass, but amplifies the grid frequency ω_o . Its purpose is to maintain a stable grid-frequency. This gives a control voltage $v_{control}(t)$ of

$$\begin{aligned} v_{control}(t) &= C'_1 \cos(\omega t - \phi_1) + C'_2 \cos(3\omega t - \phi_2) \\ &\quad + B \cdot v_{ac}(t) \end{aligned} \quad (9)$$

where C'_1 , C'_2 , B , ϕ_1 , and ϕ_2 are constants determined by $v_{in,rc}(t)$ through the RC controller. By assuming that the fundamental frequency component of $v_{ac}(t)$ has much larger amplitude than its harmonics, we can approximate that

$$v_{ac}(t) * h_{rc}(t) \approx C_{ac} \cos(\omega_o t + \phi_{ac}) \quad (10)$$

where h_{rc} is the impulse response of the RC controller, and C_{ac} and ϕ_{ac} are constant determined by $B \cdot v_{ac}(t)$ through the RC controller. As $v_{control}$ is proportional to v_{ac} we get that

$$v_{ac}(t) = C_1 \cos(\omega t - \phi_1) + C_2 \cos(3\omega t - \phi_2) \quad (11)$$

Where C_1 , C_2 , ϕ_1 , and ϕ_2 are constants determined by $v_{control}(t)$ through the dc/ac inverter. Note that the distortions in (11) is a sum of two frequency components, but is caused by a multiplication operator in the controller.

III. VALIDATION METHODOLOGY

Three sections will be presented to verify the characteristics of the output voltage $v_{ac}(t)$ as shown in sec. II and discuss its consequences. The first approach is to use the analytical expression from (11) to calculate its frequency power spectrum and Hilbert-Huang transform. Then, the result will be compared with the corresponding output voltage obtained with a Matlab Simulink model of the same system. The third step will consist of comparing the analytical and simulated models with the with the corresponding output voltage waveform measured at an operating microgrid in the field.

A. Analytical Model

Fig. 3a shows $v_{ac}(t)$ as described in (11) and an ideal ac voltage waveform as in (1) used as reference (red line). The constants in (11) is based on reasonable values of the involved system parameters. By visual inspection of $v_{ac}(t)$ we can see that it is not ideal.

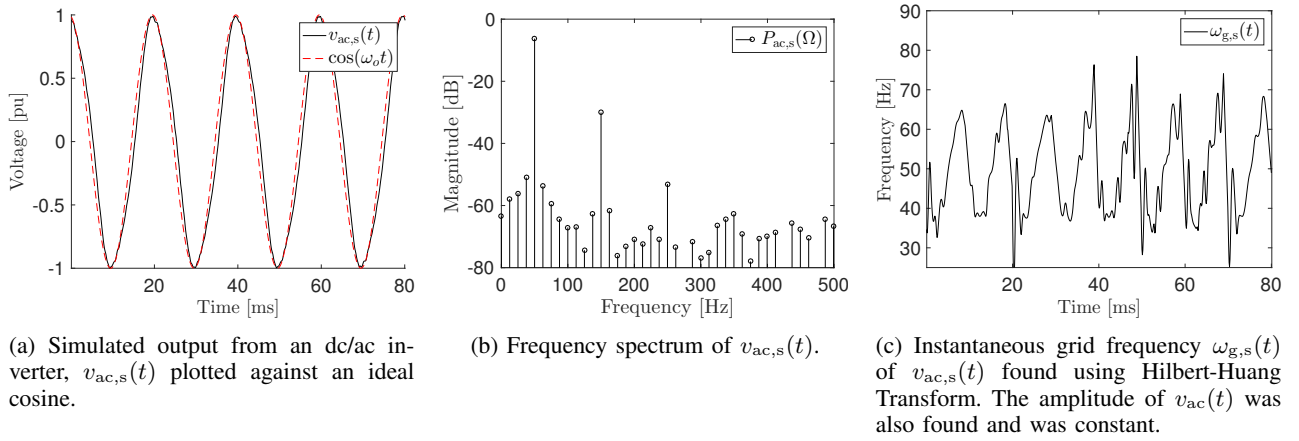


Fig. 4: $v_{ac,s}(t)$ together with its frequency power spectrum and Hilbert-Huang transform.

1) *Frequency power spectrum*: The Fourier transform is a method to decompose any time series down to sinusoidal components with constant amplitude and frequency. The discrete Fourier transform can be used to define a frequency power spectrum (periodogram) of a time series expressing the power of each frequency component. The frequency power spectrum of a sampled version of $v_{ac}(t)$ is then given by

$$P_{ac}(\Omega) = \frac{1}{N} \left| \sum_{n=0}^{N-1} v_{ac}(n \cdot T_s) e^{-j\Omega n} \right|^2 \quad (12)$$

where Ω is the angular frequency variable, T_s is the sampling period, n is the discrete time variable, and N is the total number of samples.

In fig. 3b we have the frequency power spectrum of $v_{ac}(t)$. The frequency power spectrum has a fundamental frequency ω_o , and one harmonic at $3\omega_o$. Because of this, it is expected that the frequency components ω_o and $3\omega_o$ will be dominating in the frequency power spectra of the simulated and measured ac voltage.

2) *Instantaneous Frequency*: As mentioned in sec. I, the motivation for investigating the source of the distortions was a study of electrical waveform data using the Hilbert-Huang Transform (HHT) to obtain the instantaneous frequency and amplitude of measured grid data from microgrids [4].

The instantaneous frequency is not well defined for multi-component signals [9], i.e. signals with more than one local extrema for each zero crossing. The HHT therefore decomposes a multicomponent signal down to monocomponents. For a general multicomponent signal $v(t)$ the HHT uses a method called the Empirical Mode Decomposition (EMD) to obtain the fewest monocomponents possible to describe it. These monocomponents are called Intrinsic mode functions (IMFs). A given voltage waveform v can be written as a sum of IMFs on the form

$$v(t) = v_r(t) + \sum_{i=1}^{\log_2 N} v_i(t) \quad (13)$$

where $v_i(t)$ is IMF number i that $v(t)$ consist of, and $v_r(t)$ is the residue. The residue $v_r(t)$ can be described as the offset voltage or a monotone function. A general monocomponent can be written on the form

$$v_i(t) = V_i(t) \cdot \cos(\theta_i(t)) \quad (14)$$

where the instantaneous frequency $\omega_i(t)$ for a monocomponent is defined as the rate of change of the phase $\theta_i(t)$, as shown in (15).

$$\omega_i(t) = \frac{d\theta_i(t)}{dt} \quad (15)$$

By simulating the analytical expression of $v_{ac}(t)$ we found that it satisfies the requirements for a monocomponent with a constant amplitude V_{ac} for all reasonable variables for tuning of the controller. This means that we can write $v_{ac}(t)$ on the form

$$v_{ac}(t) = V_{ac} \cos(\theta_{ac}(t)) \quad (16)$$

Since V_{ac} is constant the instantaneous frequency, $\omega_{ac}(t)$, of $v_{ac}(t)$ is unambiguous. The instantaneous frequency $\omega_{ac}(t)$ is shown in fig. 3c. From the figure it is clear that the frequency changes over time. The instantaneous frequency should ideally be $\omega_{ac}(t) = \omega_o$. We approximated $\omega_{ac}(t)$ to

$$\omega_{ac}(t) \approx \omega_o + \epsilon \cos(2\omega_o t) \quad (17)$$

with an error of less than 11.7%. The constant ϵ corresponds to the magnitude of the oscillating frequency. Although the error in (17) not neglectable, it is reasonable to expect a oscillating frequency with a periodicity of $\frac{1}{2f_o}$ in the simulations and measured voltage waveforms.

B. Analysis of microgrid simulations

A simulation of the microgrid system in fig. 2 was implemented using Simulink to verify the finding from sec. III-A. The simulation was tailored to show as real conditions as possible, and is simulating non-ideal conditions with considerable line-impedance and a resistive load as experienced in the microgrid where we did the measurements. The letter s will be added in subscript to variables to mark that they

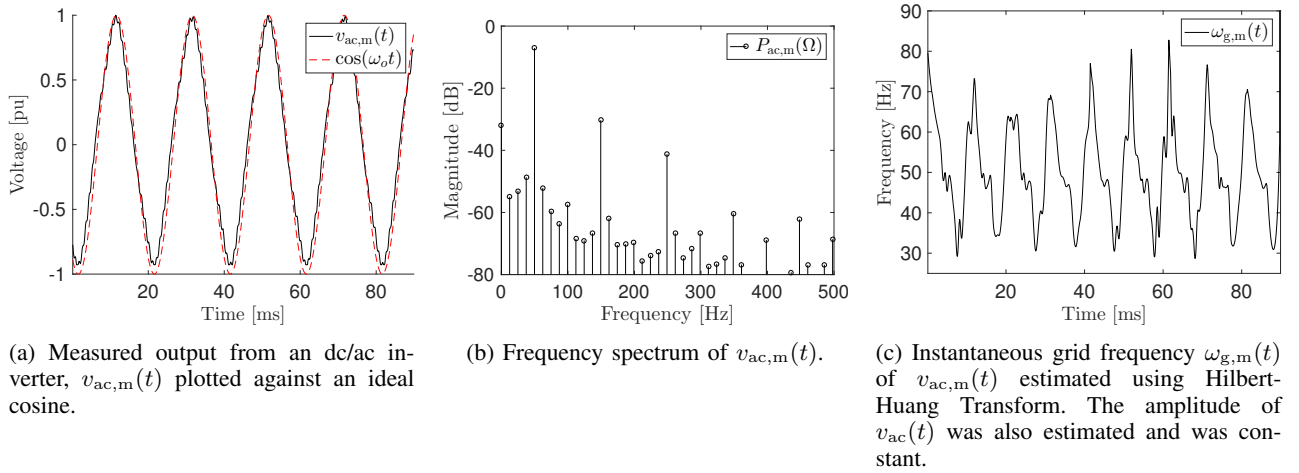


Fig. 5: $v_{ac,m}(t)$ together with its frequency power spectrum and Hilbert-Huang transform.

are found using the simulation. The ac voltage $v_{ac,s}(t)$ is shown in fig. 4a. $v_{ac,s}(t)$ is distorted compared with a pure sinusoidal waveform with frequency ω_o , yet in a different way than v_{ac} in fig. 3a. Unlike the analytical expression of v_{ac} , the ac voltage $v_{ac,s}(t)$ curves towards the right compared with a pure sinusoidal signal. It also contains ripples that are most probably caused by the distortions by the inverter's pulse-width modulation that was not properly filtered by the low-pass filter.

The frequency power spectrum of $v_{ac,s}$ is given in fig. 4b. The spectrum only shows harmonics between 0 and 500 Hz, although harmonics with higher frequencies are present. From the plot, it is easy to identify the two most significant peaks at ω_o and $3\omega_o$, especially with a prior knowledge of the distortions resulting from $v_d(t)$ and the controller. However, the frequency power spectrum does not have a significant $2\omega_o$, as in the root of the problem, given by \tilde{v}_d .

The ripples make $v_{ac,m}(t)$ a multicomponent signal, so it was decomposed into two IMFs using EMD with zero residue. One IMF contains high-frequency distortions most probably caused by non-ideal filtering of the pulse-width modulated voltage waveform. This IMF will not be further analyzed in this paper. The other monocomponent $v_{g,s}(t)$ corresponds to the grid-frequency. The monocomponent $v_{g,s}(t)$'s amplitude is constant, making its instantaneous frequency $\omega_{g,s}(t)$ unambiguous and comparable with analytical $\omega_{ac}(t)$.

Fig. 4c shows the instantaneous frequency $\omega_{g,s}(t)$, which has a semi-periodic behaviour similar to the results from sec. III-A. It has a pattern with repetitions every 10 ms, or written differently: $\frac{1}{2f_o}$. The nonperiodic parts of $\omega_{g,s}(t)$ can be caused by the nonlinear properties of the inverter, and will be the focus for future studies, once the periodic phenomena have been explained properly.

C. Analysis of Microgrid Field Measurements

The above analysis is without value if they do not correspond to the real world. Therefore, to validate the results, we

compared the analytical solution and the simulation results with the electrical voltage waveform measured on the output of a physical single-bridge inverter in an islanded microgrid, $v_{ac,m}(t)$. The microgrid used was at the The Royal University of Bhutan's College of Science and Technology, and we collected the data during operation. The microgrid provided power to their library, and the load impedance was mostly resistive. The setup in fig. 2 and the simulation is modeled after this microgrid. The measured waveform, $v_{ac,m}(t)$, is shown in fig. 5a. It is visually similar to $v_{ac,s}(t)$, except that its curving is towards the left instead of the right. It also has harmonics caused by non-ideal filtering in the inverter.

The frequency power spectrum of $v_{ac,m}(t)$ is given in fig. 5b. As in the analytical and simulated voltage waveforms, the frequency power spectrum of $v_{ac,m}(t)$ has notable peaks around ω_o and $3\omega_o$. Its harmonic at $5\omega_o$ has a larger magnitude than $v_{ac,s}(t)$'s fifth harmonic. The spectrum also contain many harmonics with higher frequencies that are not displayed in fig. 5b.

As in sec. III-B, the measured voltage waveform $v_{ac,m}(t)$ is a multicomponent signal. Like $v_{ac,s}(t)$, it was decomposed down to two IMFs. One with high-frequency distortions and the other corresponding to the grid, $v_{g,m}(t)$. The last IMF's instantaneous frequency, $\omega_{g,m}(t)$, is shown in fig. 5c.

Like v_{ac} and $v_{g,s}$, its amplitude is constant, making $\omega_{g,m}$ unambiguous. $\omega_{g,m}(t)$ has, like $\omega_{g,s}(t)$, a semi-periodic behaviour with periods of 10 ms ($\frac{1}{2f_o}$).

Based on the similarities between the analytical observations, the analysis of the simulation and the data from measured voltage waveforms in an operating microgrid, it is reasonable to say that the hypothesis proposed by the authors in previous works [4], that the semi-periodic fluctuations in the instantaneous frequency observed on microgrid data is the result of distortion $\tilde{v}_d(t)$ on the dc bus $v_d(t)$ propagating through the microgrid controller, is correct.

IV. DISCUSSION

A validation study for the relevance of the instantaneous frequency concept on electrical microgrids has been outlined in this paper. The root cause of the distortions previously detected on the microgrid and reported in this paper has been verified by analytically examining how the intrinsic oscillatory component of the dc voltage propagates through the controller feedback of the PV inverter system; resulting in an amplitude modulation, according to the analysis of the mathematical expression of the output voltage waveform of the inverter. The voltage waveforms from the analytical model, from the simulated model and from the measurement on the grid give different information about the signals depending on the method used to analyze them.

Discrete Fourier Transform based frequency power spectrum and Hilbert-Huang Transforms were used to study the results from analysis, simulation and field measurements. The frequency power spectrum of the analytical results shows two components; the one corresponding to the fundamental grid frequency (50 Hz) and a third harmonic (150 Hz). These two frequency components are also observed when the simulated and measured field data are analyzed using the frequency power spectrum. However, a clear distinction between these two frequency components was not well captured from the Fourier analysis due to, among other things, the presence of multiple frequency components in the frequency power spectrum.

When the Hilbert-Huang Transform was used to analyze the data (from analysis, simulations and field measurement), an instantaneous oscillatory frequency, with a cycle of circa 10 ms (100 Hz) was clearly identified. Although the oscillations were distorted compared with the analytical results, the instantaneous oscillatory frequency was strikingly similar. The root cause of this phenomena can be attributed to the propagation of the inherent 100 Hz oscillatory power that characterizes single phase electrical systems. It was shown in the analysis that the inverters dc bus is constrained to provide a dc current with an oscillatory component of twice the frequency of the ac current on the inverter side. This double frequency component of the current is the root of the oscillatory component observed in the dc voltage at twice the grid frequency. When this dc voltage is measured and compared with the dc reference voltage and is given as the input to the PI controller, it propagates through the inverter controller to the ac side through the pulse-width modulation. This component appears as an oscillatory frequency of the ac voltage of the inverter, as observed when analyzed with the HHT.

From the observations of these results, the authors argue that, the presence of time varying frequencies cannot not be well captured by the Discrete Fourier Transform. The Hilbert-Huang transform however, by not making any a-priori assumption of constant frequency or amplitude, is not constraining the interpretation of the data through a set of constant frequency components as Fourier does. Through the concept of instantaneous frequency defined as the derivative of the phase angle with respect to time, the HHT does not remove from the data its intrinsic attribute of instantaneous

frequency. This notion of instantaneous frequency is new in electrical systems and the case presented in this paper is an example that shows the existence of a time varying frequency caused by the control of the power electronics converter. Better understanding of this phenomena can enable more affordable diagnosis tools and reliable microgrids in rural areas.

APPENDIX A DC VOLTAGE

A. PV power source

This appendix will concern the PV power source and boost controller's output voltage and current (see fig. 2). Fig. 6a shows a Thévenin equivalent of dc power supply. By following the argumentation of Mohan et. al [6, p. 214] we get that

$$\begin{aligned} i_d(t) &= I_d + \tilde{i}_d(t) \\ &= I_d + \tilde{I}_d \cos(2\omega_o t) \end{aligned} \quad (18)$$

The simulation of the dc current $i_d(t)$ is shown in fig. 6b. \tilde{I}_d is the amplitude of $\tilde{i}_d(t)$. Equation (18) assumes that

$$V_d \gg \tilde{v}_d(t) \quad (19)$$

The dc voltage supply $v_d(t)$ will be described by

$$\begin{aligned} v_d(t) &= V_s - i_d(t) \cdot R_s \\ &= V_s - R_s \cdot I_d + R_s \tilde{I}_d \cos(2\omega_o t) \\ &= V_d + \tilde{V}_d \cos(2\omega_o t) \end{aligned} \quad (20)$$

where V_s is the constant dc power supply, R_s is the power supply's internal resistance, $V_d = V_s - R_s \cdot I_s$, and $\tilde{V}_d = R_s \tilde{I}_d$. Fig. 6c shows the simulation of the dc voltage $v_d(t)$.

ACKNOWLEDGMENT

We would also like to thank Norden Huang for personally giving insight into his methods. His open-mindedness and generosity has been highly appreciated.

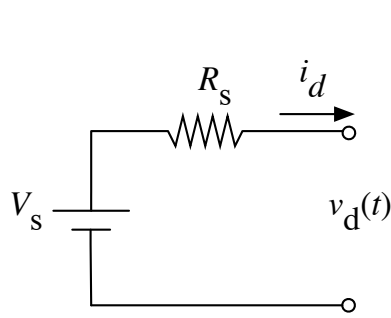
The authors would like to acknowledge the contribution of Jon Are Suul for providing a simulation setup of a single phase inverter.

Thanks are in order for Tshewang Lhendup and, Cheku Dorji and my travel partner and coworker Håkon Duus for their assistance in collecting electrical voltage waveform data.

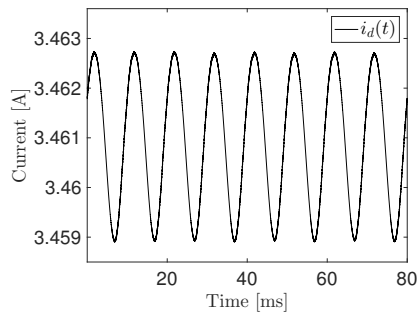
The PV icon in fig. 2 were designed by Freepik.

REFERENCES

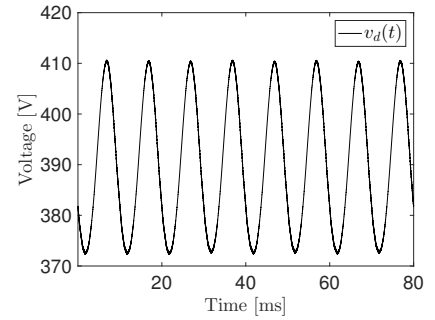
- [1] ACME Portable. Flexpac (photograph). <http://www.acmeportable.com/images/2014/11/norm-flexpac-2.jpg>. [Online; accessed 30-June-2016].
- [2] United Nations Sustainability Goals. Affordable clean energy: why it matters. http://www.un.org/sustainabledevelopment/wp-content/uploads/2016/06/Why-it-Matters_CleanEnergy_1p.pdf. [Online; accessed 30-June-2016].
- [3] International Energy Agency. About energy access. <https://www.iea.org/topics/energypoverty/>. [Online; accessed 30-June-2016].
- [4] Geir Kulia, Marta Molinas, Lars Lundheim, and Bjørn B. Larsen. Towards a real-time measurement platform for microgrids in isolated communities. *Procedia Engineering*.



(a) Thévenin equivalent of dc power supply.



(b) Simulated dc current $i_d(t)$.



(c) Simulated dc voltage $v_d(t)$.

Fig. 6: Thévenin equivalent of dc power supply and simulated dc current and voltage $i_d(t)$ and $v_d(t)$.

- [5] Norden E. Huang, Zheng Shen, Steven R. Long, Manli C. Wu, Hsing H. Shih, Quanan Zheng, Nai-Chyuan Yen, Chi Chao Tung, and Henry H. Liu. The empirical mode decomposition and the hilbert spectrum for nonlinear and non-stationary time series analysis. *Proceedings: Mathematical, Physical and Engineering Sciences*, 454(1971):903995, 1998.
- [6] William P. Robbins Ned Mohan, Tore M. Undeland. *Power electronics - Converters, Applications, and Design*. Wiley, New York, 3 edition, 2003.
- [7] Remus Teodorescu, Marco Liserre, and Pedro Rodriguez. *Grid Converters for Photovoltaic and Wind Power Systems*. Wiley, Sussex, UK, 2011.
- [8] Y. Yang, F. Blaabjerg, and H. Wang. Constant power generation of photovoltaic systems considering the distributed grid capacity. In *2014 IEEE Applied Power Electronics Conference and Exposition - APEC 2014*, pages 379–385, March 2014.
- [9] Boualem Boashash. Estimating and interpreting the instantaneous frequency of a signal - part 1: Fundamentals. *Proceedings of the IEEE*, 80(4):520–538, 1992.